Towards mass production of functionalized plastic components via multi-beam nanostructuring of moulds

P. Hauschwitz*[a]

[a] HiLASE Centre, Institute of Physics, Czech Academy of Sciences, Za Radnici 828, Dolni Brezany 25241, Czech Republic;

* Corresponding author: petr.hauschwitz@hilase.cz

ABSTRACT

Smart surface functionalization by laser-made micro and nanostructures is a suitable tool to maximize the value of a product and enable new properties for common materials. Despite the recent progress, the capacity to produce micro and nanoscale surface features over large areas represents a significant challenge in terms of production technology, throughput and cost, especially for components with a complex 3D geometry. In this work, we introduce multi-beam technologies able to efficiently micro/nanostructure metallic moulds with the ability to transfer micro/nanoscale morphology to complex 3D polymeric components via mass production techniques such as injection moulding. Moulded samples with replicated structures demonstrated advanced functional properties, including increased contact angle by 27°, bacteria reduction by 99.8% and decreased friction coefficient by 66% compared to the reference sample.

Keywords: multi-beam, injection moulding, polymers, surface functionalization, beam shaping

1. INTRODUCTION

The functionality of many industrial parts and products depends on how their surfaces interact with their surroundings. Laser structuring offers a simple contactless one-step process for controlling the surface morphology of almost arbitrary materials. Therefore, a smart surface functionalization by laser-made micro and nanostructures is a suitable tool to maximize the value of a product and enable new properties for common materials. Fine surface features have been exploited to modify friction, adhesion, wettability, optical properties, cell growth and bacterial retention [1-9].

Despite this progress, the capacity to produce micro and nanoscale surface features over large areas represents a significant challenge in terms of production technology, throughput and cost. In the last years, multi-beam technology was proven to significantly improve productivity by parallelization into more than 1000 simultaneously structuring laser beams [10-14]. However, for components with a complex 3D geometry lower number of beams or complex strategies have to be applied, which decreases the throughput. Thus, from a manufacturing point of view, the capacity to produce micro and nanoscale surface features over large and complex 3D parts represents a significant challenge.

Mass production techniques such as injection moulding are suitable for the production of functionalized 3D parts with complex 3D geometry. The ability to transfer micro and nanoscale morphology from metallic moulds to polymeric components with standard production processes greatly improves productivity and economic feasibility and was identified as the efficient and cost-effective way to produce functional micro/nanostructures [15]. This technology enables the mass production of complex polymeric components with micro- and nano-structured surfaces.

In this work, an efficient technology for mould structuring has been developed targeting efficient laser surface micro/nanostructuring with state-of-the-art precision (< 1 μm) and productivity (> 100 cm2/min). The functionality of produced structures has been tested for wettability, antibacterial and friction properties.

2. MATERIALS AND METHODS

Tool steel moulds were cleaned in ethanol prior to laser processing and treated by Ytterbium based diode-pumped solid-state laser system Perla (HiLASE, Czech Republic) emitting 1.7 ps pulses with M^2 of 1.15 and wavelength of 1030 nm [16]. The laser system can be operated at different repetition rates reaching either high average power of 200 W with a repetition rate of 50 kHz and 100 kHz or high pulse energy up to 20 mJ with 1 kHz repetition rate. To increase the efficiency during micro and nanostructuring the incident laser beam was guided into the dynamic beam shaping unit FBS G3 (Pulsar Photonics GmbH, Germany) equipped with a spatial light modulator (Hamamatsu Photonics, Japan) and galvanometer scanner (Scanlab GmbH, Germany), see Figure 1. The output beam was focused on a sample with 100 mm telecentric F-theta lens resulting in a spot diameter of 30 µm. By uploading the pre-calculated computer-generated hologram (phase-mask) on SLM the incident beam wavefront was modified resulting in the desired diffractive pattern on the sample.

The tribological properties of moulded plastic parts were tested by the pin-on-disc (ball-on-disc) method. In this method, the tested sample is rotating at a particular speed and is loaded off-axis by testing the ball using a death weight-body. The testing apparatus records the friction force, time and number of cycles continuously. An alumina (Al2O3) ball with a diameter of 6 mm was used for the analysis.

To test anti-bacterial properties, samples were disinfected by rinsing with 70% denatured ethanol. For the analysis two bacterial strains were used, gram-negative Escherichia coli (CCM 4517) and gram-positive Staphylococcus aureus (CCM 4517). Bacterial colonies were transferred into Nutrient Agar (HiMedia laboratories, India) with inoculation loops and incubated for 24 hours at 37 °C. The antibacterial testing was performed according to the article published by Lutey et al. [2].

Optical contact angle measuring device (OCA 15EC, Data Physics Instruments) was used to evaluate wettability of the treated surfaces by analyzing static contact angle under 8 µl deionized water droplets. The surface morphology was investigated by laser scanning confocal microscope, Olympus OLS5000 and scanning electron microscope, Tescan MIRA at electron energy of 15 keV.

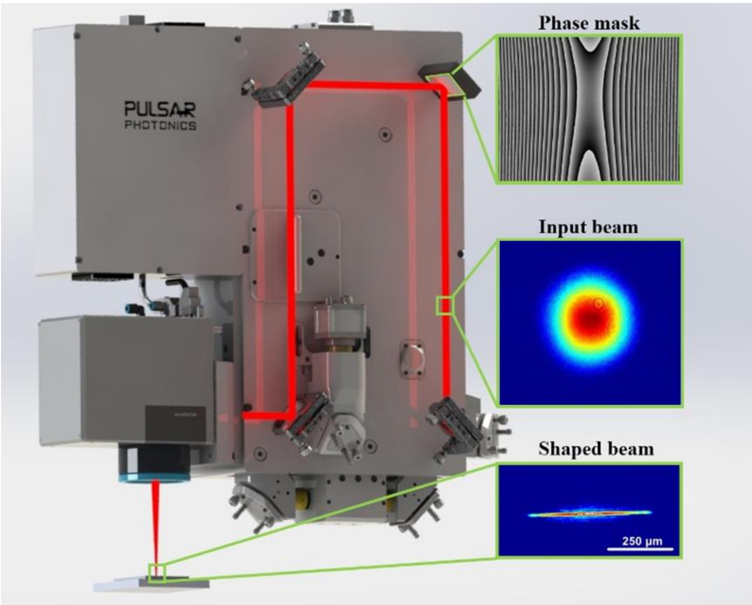

Figure 1. Schematics of beamshaping experimental setup with insets of the input beam, calculated phase mask for rectangular beam shaping and final beam shape in the image plane.

3. RESULTS AND DISCUSSION

In the first step, laser and processing parameters were optimized for the production of different kinds of micro and nanostructures as well as their combinations on the top of the mould surface. In the following step, two representative microstructures were selected for the purpose of this work – microholes with a diameter of 30 µm, depth of 50 µm (Figure 2a) and square-shaped micropillars with a side of 40 µm and height of 30 µm (Figure 2c). The production speed of these microstructures was 0.6 cm^2/min and 1 cm^2/min for the microholes and micropillars, respectively. In addition, laser-induced periodic surface structures (LIPSS) were fabricated on top of these surfaces with a productivity of 2.6 cm^2/min (Figure 2b,d,e). The periodicity of LIPSS was measured as 747 nm with a height of 300 nm.

To reach the measured depth of microholes and height of micropillars, the laser beam had to be scanned 20 times over the surface (20 overscans). Thus, to increase the microstructuring productivity, the input beam was divided by means of a dynamic beamshaping unit into a line of 20 beams. Therefore, single overscan was necessary to produce selected microstructers. The resulting productivity was 12 cm^2/min and 20 cm^2/min for the microholes and micropillars, respectively. Additionally, in case of LIPSS production the input beam was shaped into the line with dimensions of 500 µm x 30 µm (Figure 1) resulting in productivity of 105 cm^2/min.

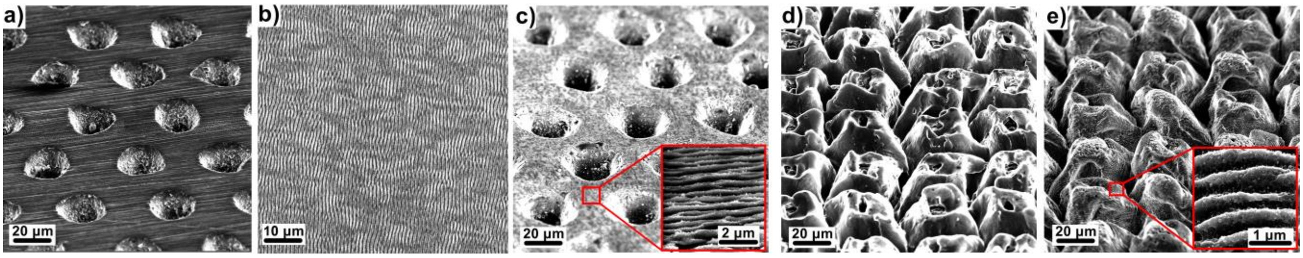

Figure 2. Structures produced on steel moulds. Insets in (b,d) shows detail of periodic nanostructure on top of the microtopography.

In the following step, mould structures were replicated on polypropylene by the injection moulding process (see Figure 3).

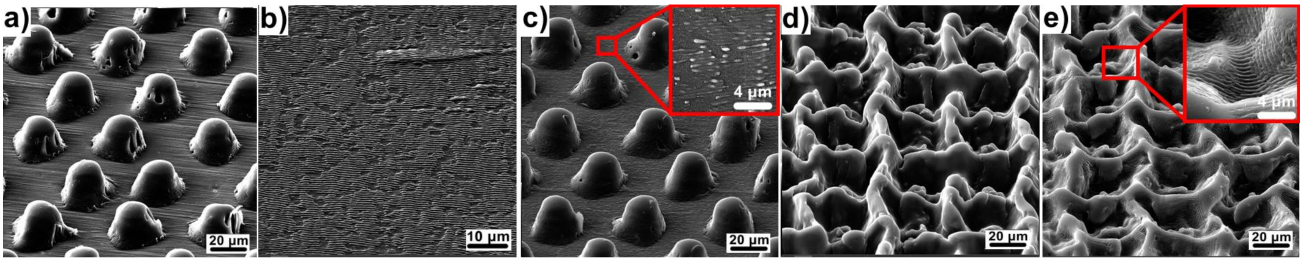

Figure 3. Replicated structures on polypropylene sample.

As can be observed in Figure 3, the replication of the hexagonal hole structure in Figure 2a resulted in the formation of round micropillars with a height of 25 µm. Therefore, the height is not reaching the bottom of the 50 µm deep hole. Figure 2b demonstrates the possibility to replicate even sub-micrometer structures as LIPSS can be observed on polypropylene surface. However, quite a large amount of defects can be observed in Figure 3b as well. Square-shaped mesh geometry can be observed on the polypropylene surface (Figure 3d) after pillar replication (Figure 2d). In this case, the height of the mesh corresponds to the height of the pillars. As shown in Figure 3c,e, replication of dual-scale structures leads to a decrease in LIPSS replication quality, compared to LIPSS on a plane surface (Figure 3b). These issues could be solved by a higher-viscosity polymer or vacuum-based injection moulding technique, which will be addressed in future work.

To demonstrate the functionality of produced surfaces, friction, wettability and bacteria adhesion properties were analyzed. The wettability of samples was evaluated by the sessile drop technique and deionized water with a droplet size of 8 µl (see Figure 4).

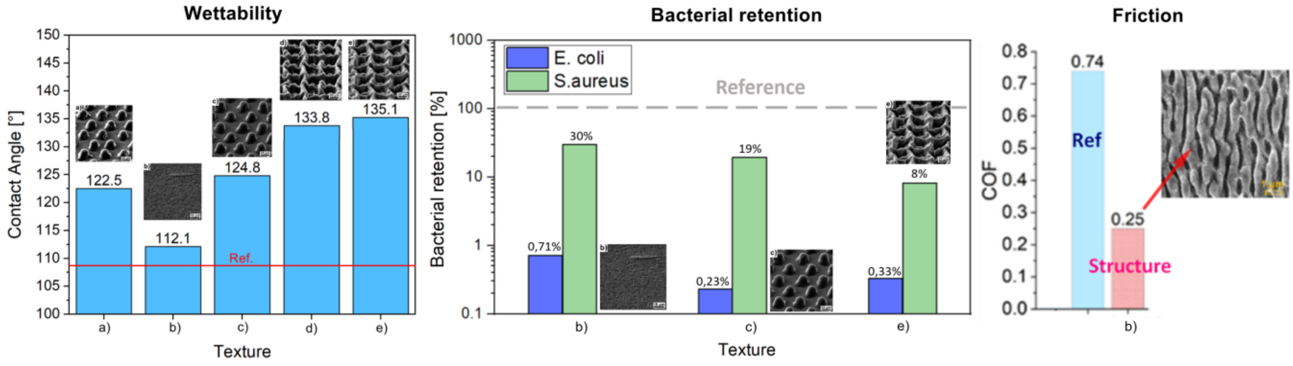

Figure 4. Analysis of functional properties of moulded polypropylene parts

As can be observed in Figure 4, all laser-treated surfaces lead to the improvement of water repellency from the original contact angle of 108°. The most significant impact on the wettability had microstructures, especially square-shaped mesh structures (Figure 3d) with a contact angle of 133.8°. Pillar microstructures increased the contact angle by 14.5° to 122.5°. Nanostructures had a minor effect increasing the contact angle by 4° when applied on a flat surface and by ~ 2° when applied on the top of microstructures. This can be explained by the LIPSS replication quality which is lower in the case of hierarchical structures. In all cases, the water droplets were pinned down having sliding angles over 80°. Therefore it is considered that the surface is in a Wenzel state [17].

In the following analysis surfaces containing LIPSS were tested for antibacterial properties. As can be observed in Figure 4, all surfaces exhibited a significant reduction in the number of living bacteria on the structured surface. Up to a 99.8% reduction in the number of bacteria was measured in the case of E. coli on the surface covered by a combination of LIPSS and micropillars and in all other cases retention of E. coli was below 1%. On the other hand, the retention of S. aureus was significantly higher, up to 30% for LIPSS on a plane surface, 19% for micropillars covered by LIPSS and 8% for the mesh structure covered by LIPSS. The higher retention for S. aureus can be explained by smaller bacterial dimensions occupying approximately 0.25 μm^2/cell compared to approximately 1 μm^2/cell occupied by E. coli. Thus, LIPSS with a periodicity of 0.75 µm cannot efficiently reduce the number of attachment points in the case of much smaller S. aureus. However, as can be observed in Figure 4, S. aureus is sensitive to wettability, as the number of cells decreases with a higher contact angle. In the final functional analysis, friction properties were tested on moulded parts covered by LIPSS (Figure 3b). As can be observed in Figure 4, it resulted in a significant reduction of the coefficient of friction by 66.2%.

4. CONCLUSION

The unique combination of high-power ultrashort pulsed laser system and flexible beam shaper resulted in efficient micro and nanostructuring of moulds. The microstructuring productivity was increased 20 times by shaping the beam into the line of 20 beams and the nanostructuring productivity was increased 40 times by shaping the beam into 0.5 mm long line. The moulding process enabled to transfer micro-, nanostructures and their combinations on to the polypropylene samples with a detail down to 750 nm. Moulded samples with replicated structures demonstrated advanced functional properties including increased contact angle by 27°, bacteria reduction by 99.8% and decreased friction coefficient by 66% compared to the reference sample. The proposed method demonstrates the possibility of efficient mass production of functionalized plastic parts.

Acknowledgements

Funding: This work was co-financed by the European Regional Development Fund and the state budget of the Czech Republic (project HiLASE CoE: Grant No. CZ.02.1.01/0.0/0.0/15_006/0000674) and from the European Union's Horizon 2020 research and innovation programme (Grant agreement NO 739573).

REFERENCES

[1] A. Rosenkranz, M. Hans, C. Gachot, A. Thome, S. Bonk, F. Mücklich, Direct laser interference patterning: tailoring of contact area for frictional and antibacterial properties, Lubricants 4(1) (2016) 2.
[2] A.H. Lutey, L. Gemini, L. Romoli, G. Lazzini, F. Fuso, M. Faucon, R. Kling, Towards laser-textured antibacterial surfaces, Scientific reports 8(1) (2018) 10112.
[3] P. Hauschwitz, R. Jagdheesh, D. Rostohar, J. Brajer, J. Kopeček, P. Jiřícek, J. Houdková, T. Mocek, Hydrophilic to ultrahydrophobic transition of Al 7075 by affordable ns fiber laser and vacuum processing, Appl. Surf. Sci. 505 (2020) 144523.
[4] J. Racek, P. Hauschwitz, R. Bičišťová, J. Brajer, J. Huyhn, P. Minárik, Laser Improved NiTi Surface for Biomedical Applications, SMST2022, ASM International, 2022, pp. 107-108.
[5] P. Hauschwitz, R. Jagdheesh, D. Rostohar, J. Brajer, J. Kopeček, P. Jiříček, J. Houdková, T. Mocek, Nanostructure fabrication on the top of laser-made micropillars for enhancement of water repellence of aluminium alloy, Materials Letters (2019) 126601.
[6] P. Hauschwitz, R. Bicistova, R. Jagdheesh, J. Brajer, D. Rostohar, Superhydrophobic stainless steel surface by two-step ns laser processing, MM Sci. J (2019) 3647-3651.
[7] I. Gnilitskyi, M. Pogorielov, R. Viter, A.M. Ferraria, A.P. Carapeto, O. Oleshko, L. Orazi, O. Mishchenko, Cell and tissue response to nanotextured Ti6Al4V and Zr implants using high-speed femtosecond laser-induced periodic surface structures, Nanomedicine: Nanotechnology, Biology and Medicine 21 (2019) 102036.
[8] P. Hauschwitz, J. Brajer, D. Rostohar, J. Kopeček, T. Mocek, M. Cimrman, M. Chyla, M. Smrž, Anti-Reflection Nanostructures on Tempered Glass by Dynamic Beam Shaping, Micromachines 12(3) (2021) 289.
[9] P. Hauschwitz, R. Jagdheesh, S. Alamri, D. Rostohar, T. Kunze, J. Brajer, J. Kopeček, T. Mocek, Fabrication of functional superhydrophobic surfaces on carbon fibre reinforced plastics by IR and UV direct laser interference patterning, Appl. Surf. Sci. (2019) 144817.
[10] P. Hauschwitz, R. Bičštová, A. Brodsky, N. Kaplan, M. Cimrman, J. Huynh, J. Brajer, D. Rostohar, J. Kopeček, M. Smrž, Towards Rapid Fabrication of Superhydrophobic Surfaces by Multi-Beam Nanostructuring with 40,401 Beams, Nanomaterials 11(8) (2021) 1987.
[11] P. Hauschwitz, J. Martan, R. Bičišťová, C. Beltrami, D. Moskal, A. Brodsky, N. Kaplan, J. Mužík, D. Štepánková, J. Brajer, LIPSS-based functional surfaces produced by multi-beam nanostructuring with 2601 beams and real-time thermal processes measurement, Scientific reports 11(1) (2021) 1-10.
[12] P. Hauschwitz, B. Stoklasa, J. Kuchařík, H. Turčičová, M. Písařík, J. Brajer, D. Rostohar, T. Mocek, M. Duda, A. Lucianetti, Micromachining of Invar with 784 Beams Using 1.3 ps Laser Source at 515 nm, Materials 13(13) (2020) 2962.
[13] P. Hauschwitz, D. Jochcová, R. Jagdheesh, M. Cimrman, J. Brajer, D. Rostohar, T. Mocek, J. Kopeček, A. Lucianetti, M. Smrž, Large-Beam Picosecond Interference Patterning of Metallic Substrates, Materials 13(20) (2020) 4676.
[14] P. Hauschwitz, D. Jochcová, R. Jagdheesh, D. Rostohar, J. Brajer, J. Kopeček, M. Cimrman, M. Smrž, T. Mocek, A. Lucianetti, Towards rapid large-scale LIPSS fabrication by 4-beam ps DLIP, Opt. Laser Technol. 133 106532.
[15] A.H. Lutey, G. Lazzini, L. Gemini, A. Peter, V. Onuseit, J. Graus, F. Fuso, R. Kling, L. Romoli, Insight into replication effectiveness of laser-textured micro and nanoscale morphology by injection molding, Journal of Manufacturing Processes 65 (2021) 445-454.
[16] M. Smrž, J. Mužík, D. Štěpánková, H. Turčičová, O. Novák, M. Chyla, P. Hauschwitz, J. Brajer, J. Kubát, F. Todorov, Picosecond thin-disk laser platform PERLA for multi-beam micromachining, OSA Continuum 4(3) (2021) 940-952.
[17] R.N. Wenzel, Resistance of solid surfaces to wetting by water, Ind. Eng. Chem. Prod. Res. Dev. 28(8) (1936) 988-994.